

MHD CHARACTERISTICS OF ASDEX H-TYPE DISCHARGES APPROACHING THE  $\beta$  LIMIT

O. Klüber, J. Gernhardt, K. Grassie, J. Hofmann, M. Kornherr, R. Stambaugh<sup>1</sup>,  
 H. P. Zehrfeld and G. Becker, H. S. Bosch, H. Brocken, A. Eberhagen,  
 G. Fussmann, O. Gehre, G.v.Gierke, E. Glock, O. Gruber, G. Haas,  
 A. Izvozchikov<sup>2</sup>, G. Janeschitz, F. Karger, M. Keilhacker<sup>3</sup>, K. Lackner,  
 M. Lenoci, G. Lisitano, F. Mast, H. M. Mayer, K. McCormick, D. Meisel,  
 V. Mertens, E. R. Müller<sup>3</sup>, H. Murmann, H. Niedermeyer, A. Pietrzyk<sup>4</sup>,  
 W. Poschenrieder, H. Rapp, H. Riedler, H. Röhr, J. Roth, F. Ryter<sup>5</sup>,  
 F. Schneider, C. Setzensack, G. Siller, P. Smeulders<sup>3</sup>, F.X. Söldner,  
 E. Speth, K.-H. Steuer, O. Vollmer, F. Wagner, D. Zasche

Max-Planck-Institut für Plasmaphysik  
 EURATOM Association, D-8046 Garching

### 1. Introduction

Due to the favourable confinement properties of the H regime,  $\beta$  values close to the Troyon limit can be achieved in the ASDEX device at a neutral injection power level  $\sim 3$  MW. In many cases, the  $\beta$  limit is a soft one, i.e.  $\beta$  attains a maximum and then decays smoothly up to the end of the injection pulse. Disruptions, however, may occur both during the rise and fall of  $\beta$ .

### 2. Temporal evolution of MHD activity in the case of soft $\beta$ limit

The investigations presented below are mainly based on the analysis of Mirnov probe signals. Due to the divertor geometry, only a fraction of the poloidal circumference could be covered, namely  $102^\circ$  at the outside and  $44^\circ$  at the inside of the torus symmetric to the midplane. The toroidal mode number  $n$  is obtained from 5 probes placed in the midplane at the outer side distributed over a toroidal angle of  $156^\circ$ . Apart from a few  $n=2$  cases not discussed in this paper, always  $n=1$  is observed.

In ohmically heated ASDEX divertor discharges, MHD activity is very weak apart from disruptive ones; in this case the common  $m = 2$ ,  $n = 1$  precursor is seen. Application of neutral beam heating at sufficient power level (maximum 3.5 MW in the case of  $H_0$  injection) leads to a continuous mode which develops during the L phase and attains a steady state lasting up to the end of the injection pulse if the discharge remains in the L regime. In the case of transition into the H-type confinement regime, however, the amplitude of the continuous mode decreases at some time after the H transition to a low level; in the further course of the discharge bursts occur as shown in Fig. 1. It is seen from Figs. 2 and 3 that these bursts have a fishbone-like character, i.e. increase and decrease of amplitude with a half-width of a few oscillations; they are referred to as fishbones in what follows.

It is well known that H-type discharges exhibit another quite different kind of MHD activity, too, namely the so-called ELMs. The most prominent manifestation of an ELM is the sudden change of the equilibrium position of the plasma column by typically a few mm (indicating a sudden decrease of the

<sup>1</sup>GA Technologies, San Diego, Calif., USA; <sup>2</sup>Academy of Sciences, Leningrad, USSR; <sup>3</sup>Present address: JET Joint Undertaking, England; <sup>4</sup>Univ. of Washington, Seattle, USA; <sup>5</sup>CEN Grenoble, France

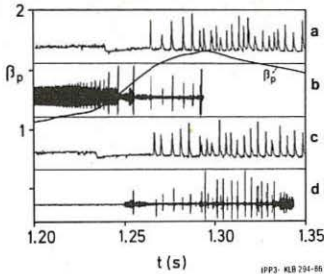


Fig. 1:  $\beta_p$ ,  $H_\alpha$  emission (traces a,c) and  $\beta_\theta$  (traces b,d) versus time for shots No. 18030 (a,b) and 18034 (c,d). Injection starts at 1.33 s and stops at 1.43 s. The temporal evolution of  $\beta_p$  is practically the same for both discharges.

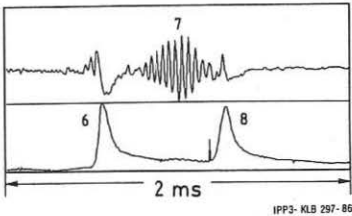


Fig. 3: Expansion of the sequence 6-7-8 from Fig. 2.

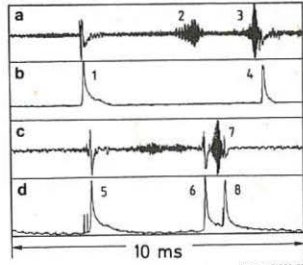


Fig. 2: Examples for ELMs (events No. 1,4,5,6,8) and fishbones (events No. 2,3,7) recorded by Mirnov probes (traces a,c) and  $H_\alpha$  monitor (traces b,d).

equilibrium parameter  $\beta_p + I_1/2$ ) and a peak in the  $H_\alpha$  emission. ELMs do not manifest, however, in the records of the Mirnov probes apart from the inward motion.

It is seen from Fig. 2 that ELMs and fishbones may occur independently from each other; on the other hand, fishbones appear to be triggered by ELMs in some cases and, more frequently, ELMs appear to be triggered by fishbones.

There are several features which are common to the continuous and the fishbone-like mode, namely

- The amplitudes measured at the outer side of the torus are much larger than those at the inner side. Amplitude ratios of 15 - 25 are typical; in many cases, the ratio must be even larger since no signals from the inner probes are obtained. Obviously, the determination of the poloidal mode number is particularly difficult in this situation.
- The frequency recorded by the soft X-ray diode cameras coincides with that of the Mirnov probe signals. During the continuous mode, an  $m = 1, n = 1$  structure with frequency doubling is clearly seen. In the case of the fishbone-like events, the amplitudes are much smaller. In some cases, doubling of frequency was observed in near-center channels which indicates that the  $q = 1$  surface may still be present.
- The mode propagates according to the toroidal rotation of the plasma applied by the unidirectional co-injection. Doppler shift measurement can only be obtained from a small zone at  $R \sim R_0 + 3a/4$ . The velocity calculated from the mode frequency is systematically by a factor of 1.4 larger than the spectroscopic one. This discrepancy increases if an additional motion of the mode due to the diamagnetic drift is assumed. Thus, the mode frequency appears to be governed by the central rotation velocity.

It is seen from Fig. 1 that the repetition rate of the ELMs does not vary appreciably during the rise and the fall of  $\beta$ . Fishbones appear more frequently in the  $\beta$  decay phase. The duration of a fishbone-like burst, however, is less than 1 ms and the island size estimated from the amplitude of  $\tilde{B}$  is typically of the order of a few cms. Hence, for this type of shots, the observed MHD activity does not explain the decay of  $\beta$ .

### 3. Discharges dominated by an $m=2, n=1$ mode

Another type is characterized by a dramatic change of the mode structure. A typical example is shown in Fig. 4. It is seen that at 1.29 s a continuous mode develops the amplitude of which increases suddenly at the inner side of the torus. A temporal expansion of this event is shown in Fig. 5. The change

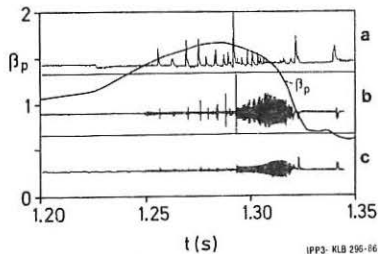


Fig. 4:  $\beta_p$  versus time for shot No. 18033. Injection starts at 1.13 s. The first disruption occurs at 1.32 s. Trace a:  $H_{\alpha}$  emission. Trace b:  $\tilde{B}_{\theta}$  from a Mirnov probe located in the midplane at the outside of the torus. Trace c: Same for the inside.

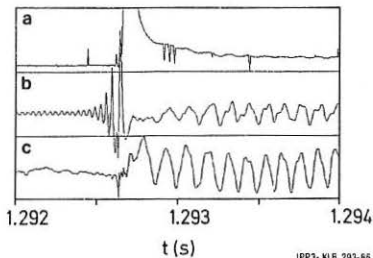


Fig. 5: Onset of the  $m=2$  oscillation in shot No. 18033. Trace a:  $H_{\alpha}$  signal (diode saturates). Trace b: Mirnov signal, midplane outside. Trace c: Mirnov signal, midplane inside. The amplitude is enhanced by a factor of 4 as compared to trace b.

of the mode structure is initiated by an ELM which is preceded by a fishbone. It is seen from Fig. 4 that the amplitude of the  $H_{\alpha}$  spike of this particular ELM exceeds by far that of the preceding and the following ones. After the transition, the mode continues to propagate in the direction given by the toroidal rotation; the frequency of it decreases, however, by a factor between 2 and 4. Most remarkably, the ratio of the frequencies before and after the transition is close to an integral number. Furthermore, it is seen that the frequency recorded before the transition remains with a small amplitude which lasts for typically 10 ms. Later on, only the "slow" mode is recorded. It is clearly an  $m = 2, n = 1$  mode, as shown in Section 4. In the case presented in Fig. 4, the  $m = 2$  mode leads to a disruption after 30 ms. In the last ms before the onset of the disruption, the signal frequency decreases drastically. In other discharges, the  $m = 2, n = 1$  mode may attain a saturated level and persist up to the end of the NI pulse. In both cases, the island size is large and may amount up to 20 % of the minor radius of the plasma column. It is seen from Fig. 4 that the onset of the  $m = 2, n = 1$  mode leads to a violent decrease of  $\beta_p$ . Most frequently, the onset of the "large"  $m = 2$  mode occurs nearly at the time at which  $\beta$  attains its maximum. In some cases, however, this mode develops already in the phase of  $\beta$  rise, in particular, if  $q_a$  is low.

#### 4. Discussion of the poloidal mode structure

In the discharges considered here, the boundary  $q$  value is  $3.5 < q_a < 4.5$ . Hence the mode numbers  $m = 2, 3$  and  $4$  (if  $q_a > 4$ ) are the candidates for the explanation of the mode structure. In a previous paper [1], one of the authors investigated the effect of the toroidal curvature on the poloidal mode structure. In this model, the modes are created by surface currents flowing on rational magnetic surfaces parallel to the magnetic field. Typical examples for the modes  $m = 2, 3$  and  $4$ ,  $n = 1$  are plotted in Fig. 6 where the phase is chosen such, that a maximum is located in the midplane at the outer side of the torus. It is seen that the amplitudes at the outer side of the torus exceed those at the inner side considerably. The amplitude ratio depends, of course, on  $\beta_p + l_i/2$ , on the aspect ratio of the resonant surfaces and on the position of the plasma column and may amount up to 5. It is further seen that the mode structure is distorted towards the inner side of the torus where the distortion is rather moderate in the case  $m=2$  but increases drastically with increasing mode number.

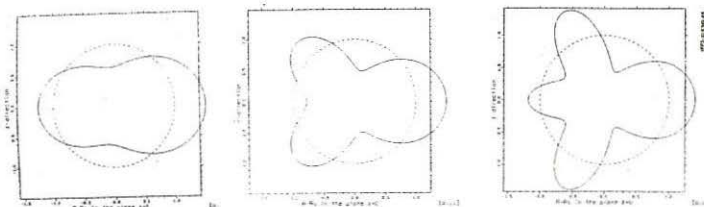


Fig. 6: Polar diagrams of the modes  $m = 2, 3, 4$ . The torus axis is on the left-hand side.

While the  $m=2$  mode discussed in the preceding section fits quite well into this picture, the continuous and the fishbone-like mode cannot be explained by this model. The observed out-in amplitude ratios of 15 - 25 might be ascribed to the occurrence of two modes, an even and an odd one, coupled such that two maxima coincide in the midplane at the outside. It is seen from Fig. 6, however, that all three modes pretend an  $m=2$  structure as far as the outer side of the torus is concerned. This contradicts to the observed phase relations according to which phase reversal is obtained at poloidal angular distances between  $45^\circ$  and  $60^\circ$  (which would indicate a superposition of  $m=3$  and  $m=4$  if the geometry were cylindrical).

Obviously, rational magnetic surfaces with  $m > 4$  are also present due to the separatrix. They are located, however, in a region with very large shear and hence very small island sizes. It is unlikely, therefore, that modes with appreciable amplitudes develop in this region.

#### 5. Summary

- Three types of MHD oscillations were observed, a continuous, a fishbone-like and an  $m=2$ ,  $n=1$  mode.
- The decay of  $\beta$  can be attributed to observable MHD activity only in the cases in which a strong  $m=2$ ,  $n=1$  mode develops.
- The continuous and the fishbone-like mode cannot be ascribed to currents flowing parallel to the magnetic field on rational surfaces.

#### Reference:

- /1/ G.Fussmann, B.J.Green, H.P.Zehrfeld, Plasma Phys.and Contr.Nucl.Fus.Res. 1980 (Proc.10th Int.Conf.Brussels, 1980), Vol.I,IAEA, Vienna (1980) 353.